Targeting pediatric cancers via T-cell recognition of the monomorphic MHC class I-related protein MR1

Annelisa M. Cornel [1,2] Loutje van der Sman,[1,2] Jip T van Dinter,[2] Marta Arrabito,[2,3] Ester Dunnebach,[1,2] Marliek van Hoesel,[1] Thomas A Kluiver,[1] Ana P Lopes,[1] Noël M M Dautzenberg,[2] Linde Dekker,[2] Jorik M van Rijn,[2] Denise A M H van den Beemt,[1] Juliane L Buhl,[2,4] Aimee du Chatinier,[2] Farnaz Barneh,[2] Yuyan Lu,[2] Luca Lo Nigro,[3] Anja Krippner-Heidenreich,[2] Zsolt Sebestyén,[1] Jurgen Kuball [1,5] Esther Hulleman,[2] Jarno Drost,[2,4] Sebastiaan van Heesch,[2] Olaf T Heidenreich,[2] Weng Chuan Peng,[2] Stefan Nierkens[1,2]

ABSTRACT

Human leukocyte antigen (HLA) restriction of conventional T-cell targeting introduces complexity in generating T-cell therapy strategies for patients with cancer with diverse HLA-backgrounds. A subpopulation of atypical, major histocompatibility complex-I related protein 1 (MR1)-restricted T-cells, distinctive from mucosal-associated invariant T-cells (MAITs), was recently identified recognizing currently unidentified MR1-presented cancer-specific metabolites. It is hypothesized that the MC.7.G5 MR1T-clone has potential as a pan-cancer, pan-population T-cell immunotherapy approach. These cells are irresponsive to healthy tissue while conferring T-cell receptor(TCR) dependent, HLA-independent cytotoxicity to a wide range of adult cancers. Studies so far are limited to adult malignancies. Here, we investigated the potential of MR1-targeting cellular therapy strategies in pediatric cancer. Bulk RNA sequencing data of primary pediatric tumors were analyzed to assess *MR1* expression. *In vitro* pediatric tumor models were subsequently screened to evaluate their susceptibility to engineered MC.7.G5 TCR-expressing T-cells. Targeting capacity was correlated with qPCR-based *MR1* mRNA and protein overexpression. RNA expression of *MR1* in primary pediatric tumors varied widely within and between tumor entities. Notably, embryonal tumors exhibited significantly lower *MR1* expression than other pediatric tumors. In line with this, most screened embryonal tumors displayed resistance to MR1T-targeting *in vitro*. MR1T susceptibility was observed particularly in pediatric leukemia and diffuse midline glioma models. This study demonstrates potential of MC.7.G5 MR1T-cell immunotherapy in pediatric leukemias and diffuse midline glioma, while activity against embryonal tumors was limited. The dismal prognosis associated with relapsed/refractory leukemias and high-grade brain tumors highlights the promise to improve survival rates of children with these cancers.

INTRODUCTION

Unconventional T-cell populations that recognize their ligand beyond the context of major histocompatibility complexes (MHC) are increasingly recognized for their potential in cellular cancer immunotherapy. Examples of unconventional T-cell populations include invariant NKT-cells (iNKT), γδ T-cells, mucosal-associated invariant T-cells (MAIT), and MR1T-cells. Unlike conventional T-cells, which rely on polymorphic MHC molecules for target recognition, these unconventional T-cells recognize their cognate target in the context of monomorphic MHC-like molecules.[1] This majorly decreases the complexity of the generation of cell therapy products suitable for individuals with diverse human leukocyte antigen (HLA) backgrounds. One interesting unconventional T-cell population is the so-called MR1T-cell population, which recognizes their cognate target in the context of MHC class I-related protein 1 (MR1).

The MHC-I-like MR1 molecule is ubiquitously expressed in most nucleated human cells.[2] Six different allelic *MR1* variants are described, of which the vast majority of the population possess the wildtype MR1*01 allele.[1] Unlike conventional MHC-I molecules, however, cell surface expression on healthy cells is low to undetectable.[3] MR1 is retained in the endoplasmic reticulum until an antigen is loaded, resulting in transient cell surface expression after dimerization with β2M.[4] MR1 complexes with intermediate metabolites produced by cells during metabolic stress, resulting in stress-induced MR1 translocation to the cell surface.[3] Until recently, MR1 was mainly considered in

association with MAIT cells. MAITs recognize intermediate metabolites derived from bacterial vitamin B2 and B9 molecules presented in MR1 to detect bacterial infection in mucosal tissues.[3 5–7]

Interest in the field of cancer immunotherapy spiked after publication of two recent studies highlighting the discovery of a distinct subpopulation of cancer-specific MR1-restricted T-cells, distinctive from MAITs.[3 6] These MR1T-cells recognize MR1-presented cancer-specific metabolite(s) on the cell surface of cancer cells, the exact nature of which remains unidentified.[8] Crowther and colleagues isolated an MR1-restricted, tumor-reactive T-cell clone from peripheral blood of a healthy donor.[6] The clone is irresponsive to healthy tissue, while conferring HLA-independent cytotoxicity towards a diverse array of adult cancer cells. They emphasize the potential of this MC.7.G5 MR1T-cell clone as a pan-cancer, pan-population T-cell immunotherapy approach.[9]

The study conducted by Crowther *et al.* thus far focused exclusively on adult malignancies.[6] Pediatric tumors exhibit distinct characteristics compared with adult tumors, including a scarcity of targetable molecules due to their low mutational burden. Consequently, there is a critical need to identify tumor-specific antigens in pediatric tumors. Even though both classified as 'cancer', it is now widely accepted that the pathobiology of pediatric tumors deviates from that of adult tumors.[10] Therefore, it remains to be studied whether the MC.7.G5 MR1T-cell clone's reactivity towards adult tumors translates to pediatric tumors. In the present study, we investigated the potential of MR1-targeted T-cell therapy in pediatric oncology using a comprehensive panel of pediatric tumor models.

METHODS
Bulk RNA sequencing
Parents of patients from whom tumors were RNA sequenced signed informed consent forms approved by the responsible authority. Sequencing library preparation and data preprocessing from fresh frozen primary tumor samples from the 812 included pediatric patients was done a priori according to the institute's standardized pipelines and guidelines.[11 12] In short, sequencing reads were aligned to the Genome Reference Consortium Human Build 38 assembly (GRCh38.p12) using STAR V.2.7.2d.[13] Duplicates were marked using the Genome Analysis Toolkit's (GATK) Picardtools V.2.20.1 MarkDuplicates. Base calling quality was reassessed with GATK V.4.2 BaseRecalibrator. Quality was assessed using Picard's CollectMultipleMetrics, EstimateLibraryComplexity and MultiQC V.1.9 was used to aggregate all reports per sample. Exons based on the GENCODE V.31 gene annotation were quantified using FeatureCounts from the Subread V.1.6.4 package[14] and normalized to gene counts per million (CPM). CPM for *MR1, HLA-A, HLA-B*, and *HLA-C* genes were retrieved via the Princess Máxima Center Biobank and Data Access Committee (BDAC) (*EGAC00001001864*). The code and data used in the analyses are available via https://github.com/VanHeeschLab/Cornel_et_al_2023.

Cell culture
In vitro pediatric cancer models, including neuroblastoma (NBL), acute myeloid leukemia (AML), B-cell/T–cell acute lymphoblastic leukemia (B-ALL, T-ALL), diffuse midline glioma (DMG), hepatocellular carcinoma (HCC), hepatoblastoma (HBL), and malignant rhabdoid tumors (MRT), were included; origin and culture conditions are summarized in table 1.[15–24] The adult chronic myeloid leukemia K562 line and adult T-ALL Jurkat line were used as a positive control.[6] *MR1* allelic variant expression of cell lines was derived from public databases (CCLE and Crown Bioscience). MR1 overexpressing cell lines were generated as described in the online supplemental methods. All cells were cultured under standard culturing conditions, refreshed and passaged biweekly, and checked every other month for mycoplasma infection and authenticity.

Generation and culturing of MC.7.G5 TCR+ T-cells
The MC.7.G5 TCR sequence was retrieved from the manuscript of Crowther and colleagues.[6] MC.7.G5 TCR expressing T-cells were generated as described in the online supplemental methods.[25–27] T-cells were stimulated once every other week using a rapid expansion protocol containing pooled irradiatedperipheral blood mononuclear cells (35 Gy), LCL-TM (80 Gy), 1 µg/mL PHA (Oxoid BV), and 50 U/mL IL-2 (Novartis) in RPMI supplemented with 5% pooled human serum and 1% P/S.[28] T-cells were phenotyped by flow cytometry after expansion to confirm stable MC.7.G5 TCR expression. T-cells were used in functional assays 10–14 days after stimulation.

Functional T-cell assays
Cytotoxicity assay
The cytotoxic capacity of MC.7.G5 TCR+ T-cells was assessed using a flow cytometry-based cytotoxicity assay. Indicated target cells were labeled with Cell-Tracer Violet (CTV) (Life Technologies) according to manufacturer's instructions. In cocultures with organoids and patient-derived xenograft cells, T-cells were labeled instead. Effects of labeling on the cytotoxic capacity of T-cells was ruled out. Cells were cocultured overnight (16–18 hours) at an effector-to-target ratio (E:T) of 10:1, unless otherwise indicated. After coculture, cells were spun down, supernatant was partly removed, and 7-AAD was added to evaluate cytotoxicity.

Cytokine secretion assay
Indicated target cells were co-cultured with MC.7.G5 TCR+ T-cells (or donor-matched, untransduced controls) overnight at an E:T of 1:1. Supernatants were harvested to determine secretion of cytokines using Legendplex according to manufacturer's instructions (Biolegend).

Table 1 List of utilized *in vitro* pediatric cancer models, culture conditions, and cell sources

In vitro model	Type of model	Culture condition	Source (identifier)
AML			
Kasumi-1	Cell lines	Standard RPMI	Princess Máxima Center (CVCL_0589)
SKNO1		RPMI+Glutamax supplemented with 20% FCS, 1% P/S and 10 ng/mL GM-CSF (Miltenyi Biotec).	Princess Máxima Center (CVCL_2196)
PDX01	PDX	PDX material derived from primary t(8;21) pediatric acute myeloid leukemia[15] was cocultured with human bone-marrow derived MSCs as feeder layer. MSCs were cultured in low glucose DMEM (Life Technologies) supplemented with 20% FCS, 8 ng/mL FGF-2 (PeproTech) and 1% P/S and were seeded in 24 well plate at a density of 7500 cell/cm2 1 day prior to PDX culture. PDX cells were then thawed and resuspended at 1×10^6 cell/mL in an in-house optimized SFEMII medium (STEMCELL Technologies) supplemented with cytokines including 150 ng/mL SCF, 100 ng/mL TPO, 10 ng/mL FLT3-L, 10 ng/mL IL-3 (all PeproTech), 1350 nM UM729 (STEMCELL Technologies), 750 nM SR1 (Biogems), and 10 ng/mL GM-CSF (Princess Máxima Center pharmacy). Cells were kept on MSCs for 3 days before cells were harvested and functional T-cell assays were performed.	Princess Máxima Center
B-ALL			
NALM6	Cell Lines	Standard RPMI	Princess Máxima Center (CVCL_0092)
RCH-ACV			Princess Máxima Center (CVCL_1851)
SUPB-15			Princess Máxima Center (CVCL_0103)
697			Princess Máxima Center (CVCL_0079)
T-ALL			
MOLT16	Cell lines	Standard RPMI	Princess Máxima Center (CVCL_1424)
CCRF-CEM			Princess Máxima Center (CVCL_0207)
HCC			
pHCC	Organoid	The culture medium was based on Saltsman *et al.*[16] with modifications as reported in[17]. The medium consisted of the following: Advanced DMEM/F12 supplemented with 1% P/S, 1% GlutaMAX, 10 mM HEPES, 1 x B27 supplement, 1x N2 supplement (all Life Technologies), 0.2% Normocin (Invivogen), 1.25 mM N-acetyl-L-cysteine, 10% (vol/vol) RSPO1 conditioned medium, 10 mM nicotinamide, 10 nM recombinant human (Leu15)-gastrin I (All Sigma), 50 ng/mL recombinant human EGF, 25 ng/mL recombinant human HGF (Both Peprotech), 10 µM forskolin, 5 µM A8301 (Both Tocris Bioscience), 10 µM Y27632 ((Abmole), and 0.5 nM WNT surrogate.[18] Cell culture and passing were performed as described by Kluiver *et al.*[19]. Basement membrane extract (BME) (R&D systems) 3D-cultures were dissociated using dispase and TripleE (both Life Technologies). Cells were washed and resuspended in the culture medium above + 2% FCS. Plates were coated with collagen I (Corning) and cells were cultured in 2D-setting before assays were initiated.	Princess Máxima Center
NBL			
GIMEN	Cell lines	DMEM+Glutamax supplemented with 10% FCS, 1% P/S, 2% non-essential amino acids (Life Technologies).	Amsterdam Medical Center (CVCL_1232)
IMR32			Princess Máxima Center (CVCL_0346)
CHP212		RPMI+Glutamax supplemented with 10% FCS, 1% P/S, 2% non-essential amino acids.	Dana Farber Institute (CVCL_1125)
SMSKAN			Dana Farber Institute (CVCL_7131)
SKNDZ			Dana Farber Institute (CVCL_1701)
NLF			Dana Farber Institute (CVCL_E217)
691b	Organoids	NBL organoids were established, characterized and cultured as described previously[20]. Organoids were maintained in DMEM low glucose, Glutamax-supplemented medium, supplemented with 25% HAM's F-12 Nutrient Mix, 2% B-27 supplement minus vitamin A, 1% N-2 Supplement, 1% P/S (all Life Technologies), 20 ng/mL Animal-Free Recombinant Human-EGF, 40 ng/mL FGF-basic, 200 ng/mL IGF-I, 10 ng/mL PDGF-AA, and 10 ng/mL PDGF-BB (all Peprotech).	Princess Máxima Center
039			
MRT			

Continued

Table 1 Continued

In vitro model	Type of model	Culture condition	Source (identifier)
78T2	Organoids	MRT organoids were established, characterized, and cultured as described previously[21] [22].	Princess Máxima Center
JD081T		In short, organoids were grown in droplets of growth factor-reduced BME type 2 (R&D Systems), advanced DMEM/F12 containing 1X GlutaMAX, 10 mM HEPES, and 1% P/S, supplemented with 10% R-spondin–conditioned medium, 1.5% B27 supplement, 50 ng/mL EGF, 50 ng/mL FGF-2 (PeproTech), 1.25 mM N-acetylcysteine, 10 mM ROCK inhibitor Y-27632, and 5 mM A83-01. Cells were cultured in 2D-setting in functional T-cell assays.	
JD041T			
60T2			
HBL			
HB13F	Organoids	HBL organoids were established, characterized, and cultured as described previously[17], see HCC for detailed culture conditions.	Princess Máxima Center
HB13E			
DMG			
JHH-DMG-01	Neurospheres	Neurospheres were established, characterized, and cultured as previously described[23][24]. Cells were maintained in DMEM/F12 and Neurobasal-A medium (1:1), supplemented with, 0.2% Primocin, 10% FCS, 1M HEPES, 1% non-essential amino acids, 1× Glutamax, 1% sodium pyruvate, 2% B-27 supplement (without vitamin A) (All Life Technologies), 20 ng/mL bFGF, 20 ng/mL EGF, 10 ng/mL PDGF-AA, 10 ng/mL PDGF-BB (All Preprotech), and 5 IE/mL Heparin (Pharmacy PMC). Biweekly, a half medium change was performed and once a week Accutase (400–600 units/mL) was used to disrupt spheres to circumvent overcrowding and necrotic core formation.	Princess Máxima Center
HSJD-DMG-07			
Adult Cancer Controls			
K562	Cell lines	Standard RPMI	UMC Utrecht (CVCL_0004)
Jurkat			UMC Utrecht (CVCL_0065)

Standard RPMI=RPMI + Glutamax (Life Technologies), supplemented with 10% FCS (Sigma)+1% Penicillin/Streptomycin (P/S) (Life Technologies).
ALL, acute lymphoblastic leukemia; AML, acute myeloid leukemia; DMG, diffuse midline glioma; HBL, hepatoblastoma; HCC, hepatocellular carcinoma; MRT, malignant rhabdoid tumor; MSCs, mesenchymal stem cells; NBL, neuroblastoma; PDX, patient-derived xenograft.

MHC-I blocking assay

MHC-I independent cytotoxicity was confirmed in an MHC-I blocking assay. 697 target cells were preincubated with 50 μg/mL panHLA-ABC blocking antibody (Clone W6/32, Biolegend) for 1 hour.[29] Cells were subsequently cultured with effector cells at an E:T of 10:1 for 5 hours. HLA-A2 restricted Wilms' Tumor 1 (WT1)-specific T-cells[30] acted as a positive control for MHC-I block. Isotype IgG antibody acted as a negative control.[29]

Flow cytometry analyses were performed on a BD FACSCanto (cytotoxicity and MHC-I blocking) or BD Fortessa (TCR expression & Cytokine Secretion Assay) (BD Biosciences). Results were standardized to cocultures with untransduced, donor-matched T-cells (online supplemental figure S3) using the formula: % cytotoxicity = (% dead cells in MC.7.G5 coculture – % dead cells in untransduced coculture)/(100 – % dead cells in untransduced coculture) × 100. Targeting was defined as >15% standardized killing. Data are shown as mean±SEM. K562 served as a positive control in all performed assays.

Quantitative real-time PCR analysis

Cells were pelleted, RNA was extracted with the RNeasy mini extraction kit (Qiagen), and cDNA was synthesized using the RevertAid H Minus First Strand cDNA Synthesis Kit with random hexamer primers (Life Technologies). mRNA expression of *MR1* was subsequently quantified using SYBR Select Master Mix (Life Technologies), the forward 5′-TAATGTGGCTCACACCATCAA-3′ and reverse 5′-GTCTTTCCCATACTCCAGGAATC-3′ *MR1* primers. Expression was determined relative to *β-actin* (forward primer: 5′-AGCGGGAAATCGTGCGTGAC-3′, reverse primer: 5′-CAATGGTGATGACCTGGC CGT-3′). Expression analysis was performed using the Quant-Studio 3 Real-Time PCR System (Life Technologies). Relative expression is visualized as $2^{-\Delta Ct}$, data shown as mean±SD.

Single cell RNA sequencing data analysis

Single cell RNA-seq data of HBL organoid models HB13E and HB13F were retrieved from and analyzed as in Kluiver and Lu *et al.*[17] The immune activation score gene signature was based on Sengupta *et al.*[31] and scores were calculated using the Seurat's AddModuleScore function.[32] Gene set enrichment analysis was performed using the fgsea package,[33] with GO Biological Process gene sets downloaded from www.gsea-msigdb.org.

Data analysis

Flow cytometric analyses were performed with FlowJo V.10.7.1. Graphs were generated using Rstudio and Graphpad Prism V.9. Differences in expression between two (embryonal vs other tumors) or more groups (different tumor entities) were evaluated using a non-parametric Mann-Whitney U or Kruskall-Wallis test between separate groups, respectively. Correlation between two genes were calculated using Pearson correlation, correlation between killing and *MR1* expression was calculated using linear regression. P values of<0.05 were considered significant.
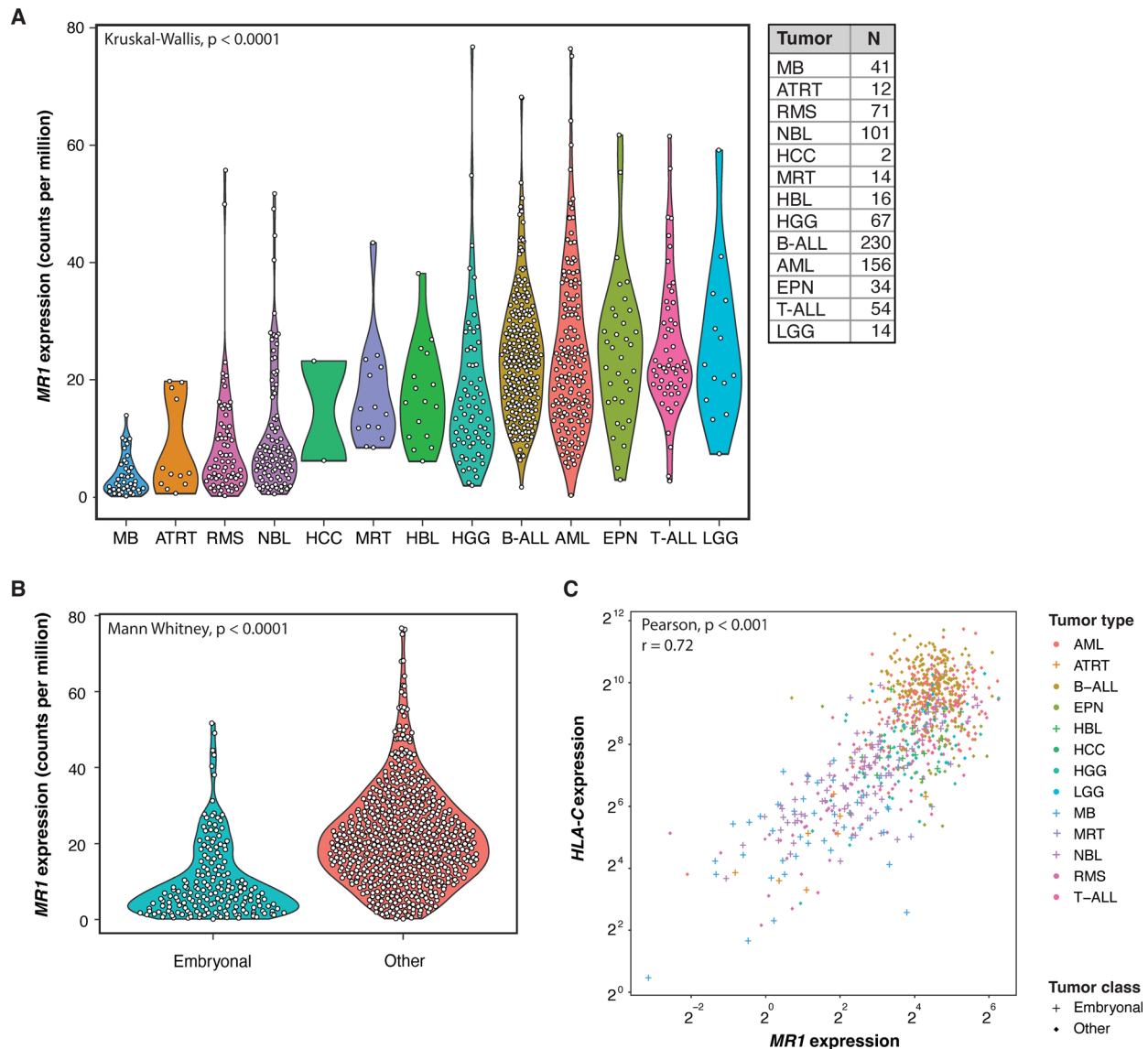
Figure 1 *MR1* mRNA expression across pediatric primary tumor entities. (A) *MR1* mRNA expression levels (counts per million) across pediatric tumor entities around diagnosis. Primary tumor biopsies are routinely bulk RNA sequenced at time of diagnosis. Statistical differences between tumor entities were calculated using a Kruskal-Wallis test. (B) *MR1* RNA expression differences (counts per million) between embryonal (MB, ATRT, MRT, NBL, and HBL) and other tumor entities. Statistical differences were calculated using a Mann-Whitney U test. (C) Correlation between *MR1* and *HLA-C* expression in pediatric primary tumors. + : embryonal tumors, • : other tumors. Log2 transformed data are shown. Correlation was determined using Pearson correlation. AML, acute myeloid leukemia; ATRT, atypical teratoid rhabdoid tumors; B-ALL, B-cell acute lymphoblastic leukemia; EPN, ependymoma; HBL, hepatoblastoma; HCC, hepatocellular carcinoma; HGG, high-grade glioma; LGG, low-grade glioma; MB, medulloblastoma; MHC-I, major histocompatibility complex I; MR1, MHC-I related protein 1; MRT, malignant rhabdoid tumors; NBL, neuroblastoma; RMS, rhabdomyosarcoma; T-ALL, T-cell acute lymphoblastic leukemia.

RESULTS

Transcriptome analysis of primary pediatric tumors reveals variable MR1 RNA expression across tumor entities

MR1 RNA expression was analyzed using bulk RNA-seq in 812 primary pediatric tumors from newly diagnosed patients. Despite the large variation in expression within and between tumor entities, significant differences in *MR1* expression were observed between tumor types (p<0.0001) (figure 1A). Across all tumors, low/high grade glioma (L/HGG), B-cell and T-cell acute lymphoblastic leukemia (B/T-ALL), acute myeloid leukemia (AML), and ependymoma expressed relatively high levels of *MR1*. Interestingly, tumors classified as embryonal (medulloblastoma (MB), atypical teratoid rhabdoid tumors (ATRT), neuroblastoma (NBL), malignant rhabdoid tumors (MRT), and hepatoblastoma (HBL)) expressed significantly lower levels of *MR1* (p<0.0001) compared with other types of tumors (figure 1B).

Embryonal tumors present in early childhood are thought to develop due to neoplastic transformation of embryonal cell stages during fetal development.[34] Many of these tumors exert low immunogenicity,[29 35–38] among

others characterized by low expression of the MHC-I coding *HLA-A/B/C* genes, which is thought to be a derivative of their origin. We determined correlation of *MR1* and *HLA-A/B/C* expression (figure 1C (*HLA-C*) and online supplemental figure S1 (*HLA-A and HLA-B*)) and observed a significant correlation between expression of these markers (r=0.71–0.72, p<0.001). This supports the hypothesis that low expression of *MR1* is part of the low immunogenic phenotype of embryonal tumors.

MC.7.G5 MR1T-cells target pediatric leukemias and glioma, but not neuroblastoma and malignant rhabdoid tumors

We next screened available *in vitro* pediatric tumor models for their susceptibility to MR1T-cell targeting. MC.7.G5 MR1T-cells were generated by lentiviral TCR introduction and variable beta chain-based FACS sorting (online supplemental figure S2A), after which functionality and MHC-I independency was confirmed in line with previously confirmed susceptibility (online supplemental figure S2B, C).[6]

Overnight coculture experiments were conducted to assess the targeting capacity of MR1T-cells in cell lines and patient-derived organoids (figure 2A). Adult leukemia lines served as positive controls (K562 and Jurkat[6]). We observed a variable targeting capacity among screened pediatric cancer models. The largest potential of MR1-directed T-cell therapy was observed in DMG and leukemic models. Both screened patient-derived DMG models were targeted by MC.7.G5 MR1T cells. Similarly, the majority of screened leukemic models demonstrated susceptibility to MC.7.G5 MR1T targeting. Interestingly, each leukemic tumor entity included one resistant model. In contrast, most of the screened NBL models (8 out of 9) and all screened MRT models were resistant to MC.7.G5 targeting. Presence of cytokines and cytotoxic granular proteins in supernatants of targeted models validated these findings (online supplemental figure S4). Consistent with the observed lower expression of *MR1* observed in embryonal tumors (figure 1), our results demonstrated that embryonal tumor models displayed significantly reduced susceptibility to MC.7.G5 MR1T-cell targeting compared with other tumor entities (figure 2B). Targeting was not restricted to an allelic *MR1* variant (online supplemental table S1).

Given the unknown MR1-presented ligand recognized by the MC.7.G5 TCR, we were unable to rely on presence of the metabolite in tumors to predict susceptibility to MC.7.G5 targeting. Therefore, we investigated whether MR1 expression could serve as a reliable marker to predict susceptibility. Since MR1 surface expression required for cancer cell recognition is below the threshold for antibody staining,[6] we quantified *MR1* mRNA expression levels and correlated this with susceptibility to MC.7.G5-mediated cytotoxicity. A significant but weak correlation (p<0.001, R^2=0.385) was observed between *MR1* expression and susceptibility to targeting (figure 2C). All tumor models with a high relative expression (>0.01) were targeted, models with a low relative *MR1* expression (<0.002) were resistant to MC.7.G5-mediated cytotoxicity. Sensitivity

of models with intermediate *MR1* expression levels was less predictive (0.002–0.01). Overall, cells susceptible to MC.7.G5 MR1T-targeting exhibited higher relative MR1 expression compared with resistant cells (p<0.001) (figure 2D).

To further substantiate the hypothesis that low *MR1* expression, and not availability of the targeted antigen, limits MC7.G5 targeting, we induced overexpression of *MR1* in three resistant tumor models (CHP212, IMR32, and CCRF-CEM) and K562 as a positive control (online supplemental figure S5). *MR1* overexpression significantly sensitized resistant models to MC.7.G5 MR1T-cell cytotoxicity (figure 2E). We next compared single cell sequencing data of the two screened HBL models that were established from the same patient, of which HB13F was susceptible to MC.7.G5 MR1T-cell targeting, while HB13E was resistant. While we observe major differences in both immunogenicity (figure 2F) and metabolic pathway enrichment (figure 2G) between the two models, we do not find enrichment of metabolic gene sets involved in nucleobase adduct generation and formation of reactive oxygen species, two processes recently suggested to be important in generation of MR1 presentable antigens[8] (online supplemental figure S6).

DISCUSSION

The recent identification of T-cells that recognize an unknown cancer-specific metabolite presented by the monomorphic MHC-I-related protein MR1 posed the question of their potential as a pan-cancer, pan-population cellular immunotherapy approach.[6] In this study, we investigated the potential of MR1-targeting cellular therapy strategies in pediatric cancer. Our findings revealed promise of targeting pediatric leukemias and brain tumors with MC.7.G5 T-cell-based immunotherapy, while targeting of embryonal cell-derived pediatric tumors was limited.

Pediatric tumors share a common low mutational burden, which critically limits the development of tumor-specific immunotherapeutic strategies.[39 40] Metabolic dysregulation is observed across all pediatric tumors, making the targeting of aberrant metabolites presented in the context of MR1 of particular interest. It is hypothesized that tumor antigens with a tumor-supporting role have the highest potential as a therapeutic target, as this could minimize the risk of immune escape due to antigen loss.[41] The CRISPR-Cas9 screen that identified MR1 specificity of the MC.7.G5 clone[6] did not yield genes related to metabolic pathway(s) involved in the generation of the unknown MR1-presented metabolite. This observation suggests that the ligand of interest is likely part of a metabolic pathway essential for cancer cell survival. Interestingly, a more recent CRISPR-Cas9 screen using several other MR1T-cell clones, found that formation of nucleobase adducts, reactive oxygen species, and carbonyl species are all important in the formation of the MR1-presented antigenic metabolite(s).[8]
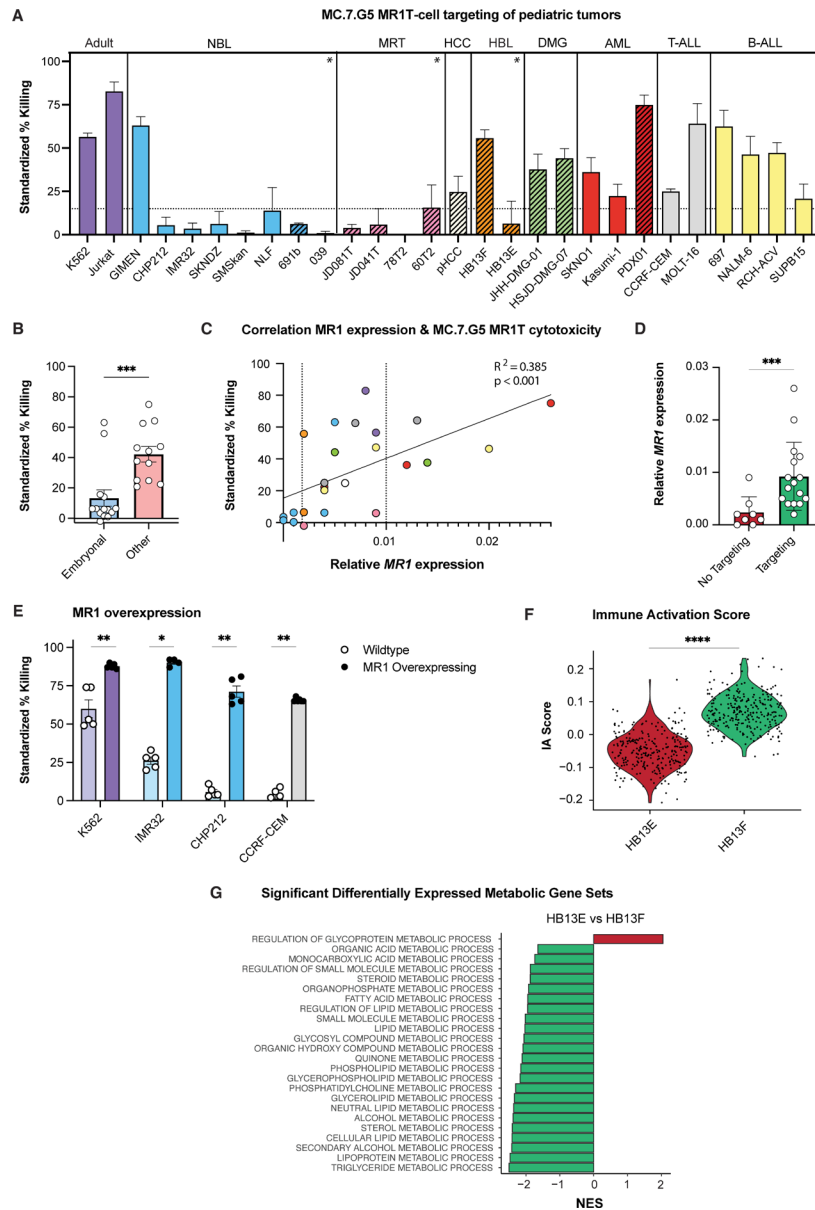
Figure 2 Heterogeneity in MC.7.G5 MR1T-cell targeting of pediatric tumor models. (A) Standardized % killing after overnight coculture of MC.7.G5 MR1T-cells at an effector-to-target ratio of 10:1 (and 1:1 for Jurkats & Nalm-6, as aspecific killing was observed in controls at higher ratios). Killing was standardized to cocultures with untransduced, donor-matched T-cells. Striped bars represent patient-derived organoid or PDX samples, filled bars represent cell lines. Tumor types marked with * are considered embryonal. K562 cells were taken along as a positive control in every assay. 039, JD081T, JD041T, 78T2: n=2, rest: n≥3. (B) Standardized % killing in embryonal tumors (MRT, NBL, and HB) compared to the other screened tumor entities. Statistical differences were calculated using a Mann-Whitney U test. ***p<0.001 (C) Correlation between standardized killing % and relative MR1 expression levels ($2^{-\Delta Ct}$) quantified by qPCR. Colors are matched to (A). Correlation was determined using simple linear regression. (D) Relative MR1 expression ($2^{-\Delta Ct}$) in MC.7.G5 targeted and non-targeted pediatric cancer models. Susceptibility to targeting was defined as >15% standardized killing. Statistical differences were calculated using a Mann-Whitney U test. **p<0.01 (E) Standardized % killing after overnight coculture of MC.7.G5 MR1T-cells with wildtype or MR1 overexpressing target cells at an effector-to-target ratio of 10:1. Killing was standardized to cocultures with untransduced, donor-matched T-cells. K562 cells were taken along as a positive control. Colors are matched to (A). n=2, five replicates. Statistical differences were calculated using a Mann-Whitney U test. *p<0.05, **p<0.01 (F) Immune activation score[31] calculated from single cell RNAseq data from MC.7.G5-resistant HB13E and MC.7.G5-sensitive HB13F HBL cells. Statistical differences were calculated using a Mann-Whitney U test.****p<0.0001 (G) Gene set enrichment analysis of gene sets involved in metabolism comparing single cell sequencing data from MC.7.G5 resistant HB13E and MC.7.G5 sensitive HB13F HBL organoids. Significantly enriched processes are shown (p<0.05). AML, acute myeloid leukemia; B-ALL, B-cell acute lymphoblastic leukemia; DMG, diffuse-midline glioma (a type of high-grade glioma); HB, hepatoblastoma; MRTs, malignant rhabdoid tumors; NBL, neuroblastoma; PDX, patient-derived xenograft; T-ALL, T-cell acute lymphoblastic leukemia.

The current study indicates that embryonal tumors, characterized by a low immunogenic phenotype,[29 35–38] also have low or absent MR1 expression. This limits the applicability of MR1-targeting immunotherapies in embryonal tumors. Nonetheless, the fact that two of the screened embryonal tumor models (GIMEN and HB13F) are susceptible to MC.7.G5 targeting does suggest the potential of inducing MR1 presentation in these tumor types. Interestingly, the GIMEN cell line is the only model out of the eight screened NBL models that reflects the mesenchymal NBL cell lineage,[42] which is reported to be more immunogenic than adrenergic counterparts.[29 31] In addition, we previously established two different hepatoblastoma organoid models using tumor tissue from the same patient.[17] The HB13F organoid, which resembles the more differentiated fetal HBL tumor subtype,[43] is susceptible to MC7.G5 targeting, while HB13E model, resembling the poorly differentiated embryonal HBL tumor subtype,[43] is resistant to such targeting. The targeting potential in a subset of embryonal tumors indicates the opportunity to induce susceptibility to MR1-restricted immunotherapeutic strategies. The fact that both MR1T-sensitive and MR1T-resistant cancer cells can be isolated from the same patient does, however, warrant studying of MR1 downregulation as a resistance mechanism against MR1-based immunotherapies.

It should be noted that the MC.7.G5 sensitivity of leukemic models was variable. This may be resulting from the stage of hematopoiesis from which the leukemic cells arose. The resistant Kasumi-1 line, for example, arose from very early myeloid stem cells that may lack immunological features like MR1 expression.[44] This further substantiates the hypothesis that the low immunogenicity of embryonal tumors causes a lack of susceptibility to MR1-mediated cytotoxicity. Future studies into cancer-specific MR1-targeting immunotherapy strategies should focus on stratification of subtypes of tumor entities susceptible to MR1T targeting. This will help to identify the specific tumor subtypes that would benefit from MR1-targeting immunotherapies.

We studied the correlation between *MR1* mRNA levels and sensitivity to targeting by the MC.7.G5 TCR to determine whether targeting efficacy could be predicted. Although the correlation was significant, the data indicate that mRNA expression of *MR1* is not the only prerequisite for efficient targeting. Overexpression of *MR1* in resistant cell lines, however, did sensitize cells to MC7.G5 cytotoxicity, indicating that the targeted antigen is present in these resistant models. Unraveling the presented metabolite(s)[8] to MR1T is key to efficiently predict, and potentially pharmacologically increase, sensitivity to MR1T-cell cytotoxicity.

Recent studies found several single nucleotide polymorphisms (SNPs) in the *MR1* gene, generating six different allelic *MR1* variants.[1] One of these SNPs, present in the *MR1*04* allelic variant represented in 1% of the population, diminishes loading of the MAIT ligand 5-(2-oxopropylideneamino)-6-D-ribitylaminouracil.[45] This indicates

that MR1 is not as monomorphic as previously assumed, which may have implications for the pan-population applicability of MR1T-based immunotherapies. A recent study suggests that a murinized version of the MC.7.G5 TCR may preferentially recognize ligand loaded *MR1*04* complexes, also on healthy B-cells and monocytes of *MR1*04* individuals.[46] Consequently, it is important to study on-target and off-target reactivity of MR1T-based immunotherapies in tumor and healthy tissue of individuals with the several *MR1* allelic variants. The fact that we and/or Crowther and colleagues show reactivity of the MC.7.G5 clone against *MR1*01* (71% population), *MR1*02* (25% population), and *MR1*04* (1% population) expressing cancer cells indicates on-target reactivity of the clone across several allelic variants.[6 46]

In conclusion, while MR1T-cell therapy may not be universally applicable to all pediatric cancers, it holds significant potential for the treatment of various pediatric tumor types. Future studies should particularly focus on the potential of MR1 targeting therapy in patients with relapsed/refractory AML and T-ALL, DMG, and ependymoma, as these patients currently have a dismal prognosis. The unique features of MR1, including its relatively monomorphic nature, widespread expression in various pediatric tumors, and the tumor-specific metabolic disruption targeted by MR1T-cells, highlight the promise of MR1T-based cellular therapy as a cost-effective approach to improve the survival rates of children with cancer.

Author affiliations

[1]Prinses Maxima Centrum voor Kinderoncologie, Utrecht, The Netherlands
[2]Center for Translational Immunology, UMC Utrecht, Utrecht, The Netherlands
[3]Center of Pediatric Hematology & Oncology, University of Catania, Catania, Italy
[4]Oncode Institute, Utrecht, The Netherlands
[5]Department of Hematology, UMC Utrecht, Utrecht, The Netherlands

ORCID iDs
Annelisa M. Cornel http://orcid.org/0000-0001-8349-121X
Jurgen Kuball http://orcid.org/0000-0002-3914-7806

REFERENCES

1 Rozemuller E, Eckle SBG, McLaughlin I, *et al*. MR1 encompasses at least six allele groups with coding region alterations. *HLA* 2021;98:509–16.
2 Riegert P, Wanner V, Bahram S. Genomics, isoforms, expression, and phylogeny of the MHC class I-related MR1 gene. *J Immunol* 1998;161:4066–77.
3 Lepore M, Kalinichenko A, Calogero S, *et al*. Functionally diverse human T cells recognize non-microbial antigens presented by MR1. *Elife* 2017;6:e24476.
4 Lamichhane R, Ussher JE. Expression and trafficking of MR1. *Immunology* 2017;151:270–9.
5 Vacchini A, Chancellor A, Spagnuolo J, *et al*. MR1-restricted T cells are unprecedented cancer fighters. *Front Immunol* 2020;11:751.
6 Crowther MD, Dolton G, Legut M, *et al*. Genome-wide CRISPR–Cas9 screening reveals ubiquitous T cell cancer targeting via the monomorphic MHC class I-related protein MR1. *Nat Immunol* 2020;21:178–85.
7 Flores-Villanueva P, Sobhani N, Wang X, *et al*. MR1-restricted T cells in cancer immunotherapy. *Cancers (Basel)* 2020;12:2145.
8 Vacchini A, Yang Q, Chancellor A, *et al*. Nucleobase adduct-containing metabolites are MR1 ligands that stimulate self-reactive MR1t cells. *BioRxiv* 2022.
9 Crowther MD, Sewell AK. The burgeoning role of MR1-restricted T-cells in infection, cancer and autoimmune disease. *Curr Opin Immunol* 2021;69:10–7.
10 Kattner P, Strobel H, Khoshnevis N, *et al*. Compare and contrast: pediatric cancer versus adult malignancies. *Cancer Metastasis Rev* 2019;38:673–82.
11 Kerstens HH, Hehir-Kwa JY, van de Geer E, *et al*. Trecode: a FAIR ECO-system for the analysis and archiving of omics data in a combined diagnostic and research setting. *BioMedInformatics* 2023;3:1–16.
12 van Belzen IAEM, Cai C, van Tuil M, *et al*. Systematic discovery of gene fusions in pediatric cancer by integrating RNA-Seq and WGS. *BMC Cancer* 2023;23:618.
13 Dobin A, Davis CA, Schlesinger F, *et al*. STAR: ultrafast universal RNA-Seq aligner. *Bioinformatics* 2013;29:15–21.
14 Liao Y, Smyth GK, Shi W. Featurecounts: an efficient general purpose program for assigning sequence reads to genomic features. *Bioinformatics* 2014;30:923–30.
15 Kellaway SG, Potluri S, Keane P, *et al*. Leukemic stem cells hijack lineage inappropriate signalling pathways to promote their growth. *BioRxiv* 2023.
16 Saltsman JA, Hammond WJ, Narayan NJC, *et al*. A human organoid model of aggressive hepatoblastoma for disease modeling and drug testing. *Cancers (Basel)* 2020;12:1–18.
17 Kluiver TA, Lu Y, Schubert SA, *et al*. Multi-dimensional profiling of hepatoblastomas and patient-derived tumor organoids uncovers tumor subpopulations with divergent WNT activation profiles and identifies pan-hepatoblastoma drug sensitivities. *BioRxiv* 2023.
18 Miao Y, Ha A, de Lau W, *et al*. Next-generation surrogate Wnts support organoid growth and deconvolute frizzled pleiotropy in vivo. *Cell Stem Cell* 2020;27:840–851.
19 Kluiver TA, Kraaier LJ, Peng WC. Long-term expansion of murine primary hepatocyte organoids. *Methods Mol Biol* 2022;2544:1–13.
20 Bate-Eya LT, Ebus ME, Koster J, *et al*. Newly-derived neuroblastoma cell lines propagated in serum-free media recapitulate the genotype and phenotype of primary neuroblastoma tumours. *Eur J Cancer* 2014;50:628–37.
21 Calandrini C, van Hooff SR, Paassen I, *et al*. Organoid-based drug screening reveals neddylation as therapeutic target for malignant rhabdoid tumors. *Cell Reports* 2021;36:109568.
22 Calandrini C, Schutgens F, Oka R, *et al*. An organoid biobank for childhood kidney cancers that captures disease and tissue heterogeneity. *Nat Commun* 2020;11:1310.
23 Taylor IC, Hütt-Cabezas M, Brandt WD, *et al*. Disrupting NOTCH Slows diffuse intrinsic pontine glioma growth, enhances radiation sensitivity, and shows combinatorial efficacy with bromodomain inhibition. *J Neuropathol Exp Neurol* 2015;74:778–90.
24 Vinci M, Burford A, Molinari V, *et al*. Functional diversity and cooperativity between subclonal populations of pediatric glioblastoma and diffuse intrinsic pontine glioma cells. *Nat Med* 2018;24:1204–15.
25 Lo Presti V, Cornel AM, Plantinga M, *et al*. Efficient lentiviral transduction method to gene modify cord blood CD8+ T cells for cancer therapy applications. *Mol Ther Methods Clin Dev* 2021;21:357–68.
26 Zufferey R, Dull T, Mandel RJ, *et al*. Self-inactivating lentivirus vector for safe and efficient in vivo gene delivery. *J Virol* 1998;72:9873–80.
27 Dull T, Zufferey R, Kelly M, *et al*. A third-generation lentivirus vector with a conditional packaging system. *J Virol* 1998;72:8463–71.
28 Marcu-Malina V, Heijhuurs S, van Buuren M, *et al*. Redirecting AβT cells against cancer cells by transfer of a broadly tumor-reactive ΓδT-cell receptor. *Blood* 2011;118:50–9.
29 Cornel AM, Dunnebach E, Hofman DA, *et al*. Epigenetic modulation of neuroblastoma enhances T cell and NK cell immunogenicity by inducing a tumor-cell lineage switch. *J Immunother Cancer* 2022;10:e005002.
30 Plantinga M, Lo Presti V, de Haar CG, *et al*. Clinical grade production of Wilms' Tumor-1 loaded cord blood-derived dendritic cells to prevent relapse in pediatric AML after cord blood transplantation. *Front Immunol* 2020;11:559152.
31 Sengupta S, Das S, Crespo AC, *et al*. Mesenchymal and adrenergic cell lineage States in neuroblastoma possess distinct immunogenic phenotypes. *Nat Cancer* 2022;3:1228–46.
32 Hao Y, Hao S, Andersen-Nissen E, *et al*. Integrated analysis of multimodal single-cell data. *Cell* 2021;184:3573–3587.
33 Korotkevich G, Sukhov V, Budin N, *et al*. Fast gene set enrichment analysis. *BioRxiv* 2021.
34 Custers L, Paassen I, Drost J. In vitro modeling of embryonal tumors. *Front Cell Dev Biol* 2021;9:1–9.
35 Yarmarkovich M, Maris JM. When cold is hot: immune checkpoint inhibition therapy for rhabdoid tumors. *Cancer Cell* 2019;36:575–6.
36 Garancher A, Suzuki H, Haricharan S, *et al*. Tumor necrosis factor overcomes immune evasion in P53-mutant medulloblastoma. *Nat Neurosci* 2020;23:842–53.
37 Marquardt V, Theruvath J, Pauck D, *et al*. IMMU-19. HDAC inhibitors sensitize MYC-amplified medulloblastoma to immunotherapy by activating the NF-KB pathways. *Neuro-Oncology* 2020;22:iii363–4.
38 Custers L, Khabirova E, Coorens THH, *et al*. Somatic mutations and single-cell transcriptomes reveal the root of malignant rhabdoid tumours. *Nat Commun* 2021;12:1407.
39 Gröbner SN, Worst BC, Weischenfeldt J, *et al*. The landscape of genomic alterations across childhood cancers. *Nature* 2018;555:321–7.
40 Ma X, Liu Y, Liu Y, *et al*. Pan-cancer genome and transcriptome analyses of 1,699 paediatric leukaemias and solid tumours. *Nature* 2018;555:371–6.
41 Beatty GL, Gladney WL. Immune escape mechanisms as a guide for cancer immunotherapy. *Clin Cancer Res* 2015;21:687–92.
42 van Groningen T, Koster J, Valentijn LJ, *et al*. Neuroblastoma is composed of two super-enhancer-associated differentiation States. *Nat Genet* 2017;49:1261–6.
43 Ranganathan S, Lopez-Terrada D, Alaggio R. Hepatoblastoma and pediatric hepatocellular carcinoma: an update. *Pediatr Dev Pathol* 2020;23:79–95.
44 Asou H, Tashiro S, Hamamoto K, *et al*. Establishment of a human acute myeloid leukemia cell line (Kasumi-1) with 8;21 chromosome translocation. *Blood* 1991;77:2031–6.
45 Howson LJ, Awad W, von Borstel A, *et al*. Absence of mucosal-associated invariant T cells in a person with a homozygous point mutation in MR1. *Sci Immunol* 2020;5:eabc9492.
46 Cornforth TV, Moyo N, Cole S, *et al*. Conserved allomorphs of MR1 drive specificity of MR1-restricted TCRs. *BioRxiv* 2023.
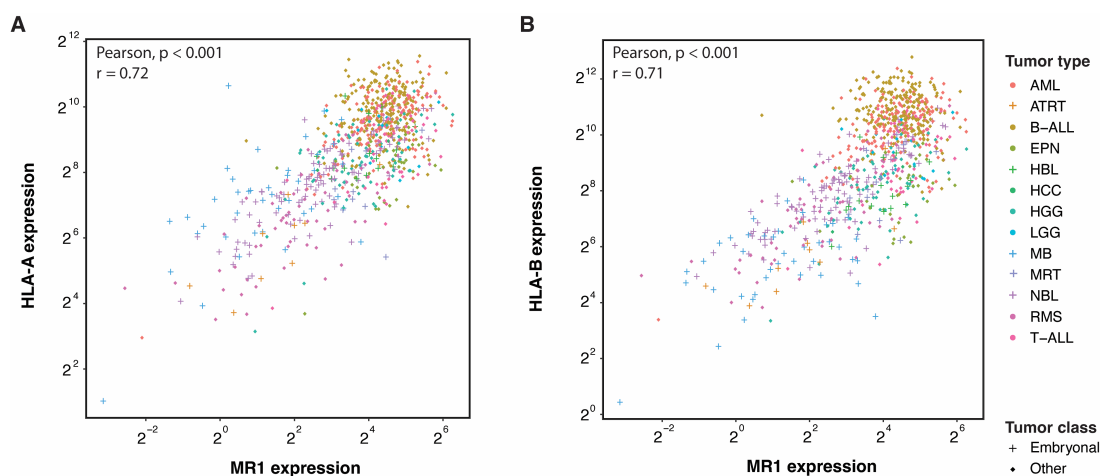
1   **Supplementary Methods**

2   *Generation of MR1 overexpressing cell lines*

3   The *MR1* transgene was synthesized (Genscript) and cloned into the pCCL-cPPT-hPGK-ORF-bPRE4-SIN

4   lentiviral transfer vector[36]. Lentiviral particles were produced using standard calcium phosphate

5   transfection (Clontech) of HEK-293T-cells with the pMDL-g/pRRE, pMD2-VSVg, and pRSV-Rev

6   plasmids[37,38]. Transducing units per mL of concentrated vector batches were determined using

7   serial dilution on Jurkat cells followed by flow cytometric analysis of MR1 expression (anti-MR1 APC

8   (8F2.F9, Biolegend)). Cells were transduced at a multiplicity of infection (MOI) of 2.5 and FACS-sorted

9   on MR1 expression (Sony SH800S Cell Sorter) (**Supplementary Figure 5**).

10   *Generation of MC.7.G5 TCR expressing T-cells*

11   The MC.7.G5 TCR sequence was obtained from the manuscript of Crowther and colleagues[5]. A furin

12   cleavage site was inserted upstream of a T2A sequence linking the TCR beta and alpha chains. The gene

13   was synthesized (Genscript) and cloned into the pCCL-cPPT-hPGK-ORF-bPRE4-SIN lentiviral transfer

14   vector[36]. Lentiviral particles were produced using standard calcium phosphate transfection

15   (Clontech) of HEK-293T-cells with the pMDL-g/pRRE, pMD2-VSVg, and pRSV-Rev plasmids[37,38].

16   Transducing units per mL of concentrated vector batches were determined using serial dilution on

17   Jurkat cells followed by flow cytometric analysis of Vβ11 expression (anti-Vβ11 FITC (KT11, Biolegend)).

18   Cord blood (CB) from healthy donors was collected under informed consent in accordance with the

19   Declaration of Helsinki, and collection protocol approved by the Ethical Committee of the UMC

20   Utrecht. CB mononuclear cells were isolated through Ficoll-Paque PLUS separation (GE Healthcare

21   Biosciences AB), after which CD8$^+$ T-cells were separated using magnetic bead separation (Miltenyi

22   Biotec). CD8$^+$ T-cells were stimulated and transduced at an MOI of 10 according to a previously

23   described protocol[36]. 7-10 days after transduction, cells were FACS-sorted on Vβ11 expression (BD

24   FACSAria II), using a panel of anti-Vβ11 FITC, anti-CD3 BV510 (Biolegend, OKT3), anti-CD8 APC (RPA-

25   T8, BD Biosciences), and 7-AAD (BD Biosciences).

Supplemental material

BMJ Publishing Group Limited (BMJ) disclaims all liability and responsibility arising from any reliance placed on this supplemental material which has been supplied by the author(s)

J Immunother Cancer

26 **Supplementary Figures**

27

28 **Supplementary Figure 1.** *MR1* expression correlates with *HLA-A* and *HLA-B* expression in primary pediatric tumor

29 samples.

30 *Correlation between MR1 and HLA-A (A) and HLA-B (B) in pediatric primary tumors. + : embryonal tumors, □:*

31 *other tumors. Log2 transformed data is shown. Correlation was determined using Pearson correlation.*
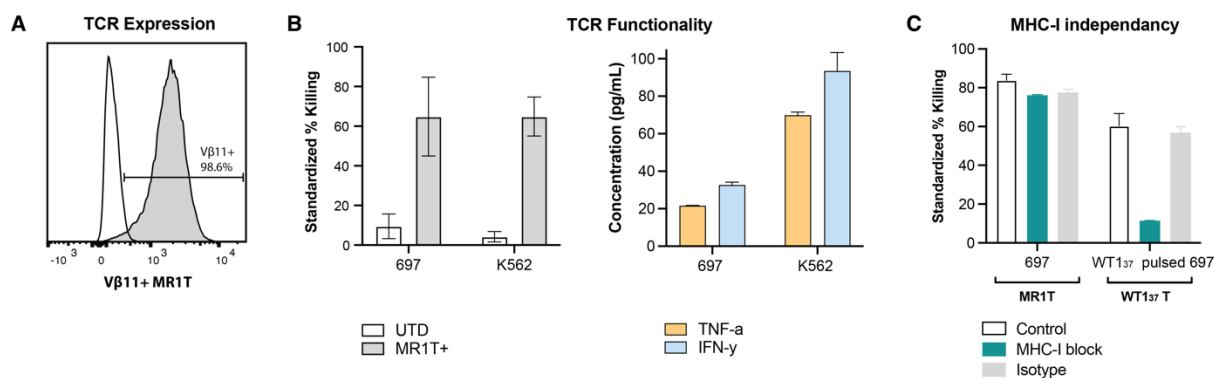
32 **Supplementary Figure 2**. Generated engineered CD8+ MC.7.G5 MR1T-cells are functional.

33 *(A) TCR expression in transduced, FACS-sorted T-cells (grey) compared to untransduced, donor-matched cells*

34 *(white). TCR expression was determined using variable beta chain 11 (Vβ11) expression. (B) Left: TCR functionality*

35 *was determined in an overnight killing assay at an effector-to-target (E:T) ratio of 10:1. Standardized % of killing*

36 *of MC.7.G5 MR1T-cells (grey) and untransduced, donor-matched counterparts (white) during co-culture with 697*

37 *and K562 target cells. Killing was standardized to target only wells, 697: n=3, K562: n=4. Right: TNFα and IFNγ*

38 *secretion (in pg/mL) was determined in overnight cultures at an E:T of 1:1. Secretion in co-cultures with*

39   *untransduced T-cells was under the detection limit, n=2 per cell line. (C) Standardized killing % of MC.7.G5 T-cells*

40   *in a 5h co-culture at an E:T of 10:1 when MHC-I mediated cytotoxicity is blocked using a panHLA-ABC blocking*

41   *antibody. MHC-I dependent WT1$_{37}$-specific T-cells function as a positive control for MHC-I block, an IgG isotype*

42   *antibody acted as a negative control.*

Non-specific targeting of untransduced T-cells
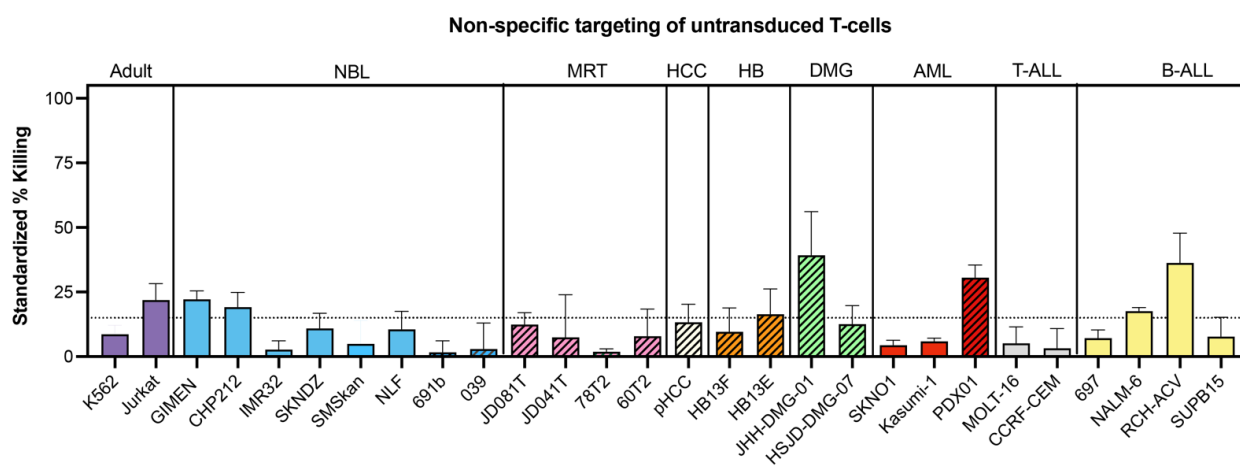
43   **Supplementary Figure 3.** Non-specific targeting of untransduced, donor-matched control T-cells

44   *Standardized % of killing after overnight co-culture of untransduced T-cells, matched to the utilized MC.7.G5*

45   *MR1T-cells, at an effector-to-target ratio of 10:1 (and 1:1 for Jurkats & Nalm-6, as aspecific killing was observed*

46   *in controls at higher ratios). Killing was standardized to wells with target only. Striped bars represent patient-*

47   *derived organoid or PDX samples, filled bars represent cell lines. Co-culture with K562 cells was taken along as a*

48   *positive control in every assay. 039, JD081T, JD041T, 78T2: n=2, rest: n≥3. NBL: neuroblastoma, MRT: malignant*

49   *rhabdoid tumors, HBL: hepatoblastoma, DMG: diffuse-midline glioma (a type of high-grade glioma), AML: acute*

50   *myeloid leukemia, T-ALL: T-cell acute lymphoblastic leukemia, B-ALL: B-cell acute lymphoblastic leukemia.*

Supplemental material

BMJ Publishing Group Limited (BMJ) disclaims all liability and responsibility arising from any reliance placed on this supplemental material which has been supplied by the author(s)

J Immunother Cancer

51
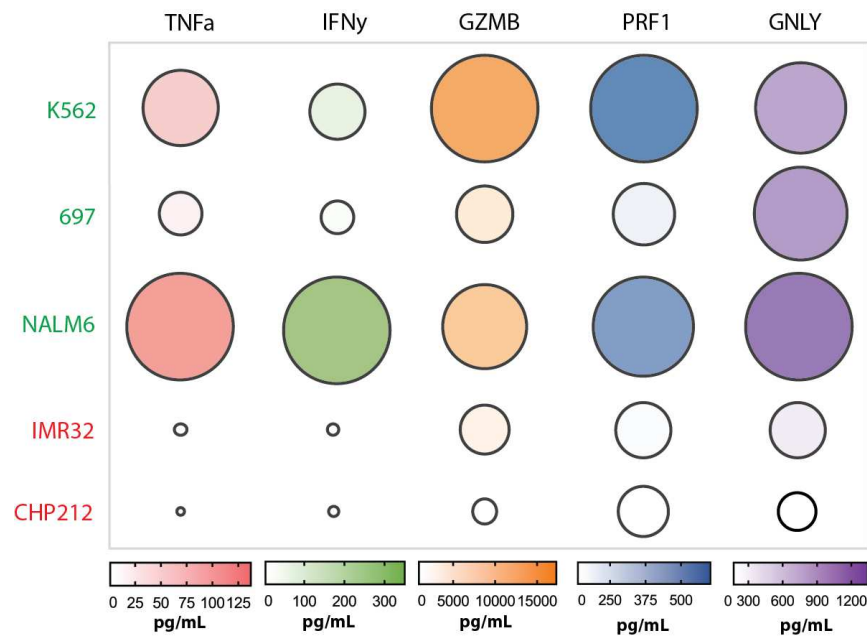
Supplementary Figure 4. MC.7.G5 MR1T-cells secrete cytokines and cytotoxic granular proteins in co-cultures with targeted cell lines.

Secretion of TNFα (red), IFNy (green), granzyme B (GZMB) (orange), Perforin-1 (PRF1) (blue), and Granulysin (GNLY) (purple) in pg/mL in co-cultures after overnight incubation at an effector-to-target ratio (E:T) of 1:1, standardized to untransduced control cells. Two MC.7.G5 sensitive cell lines (697 and NALM6) and two resistant cell lines (IMR32 and CHP212) were analyzed in duplicate, K562 co-cultures were taken along as a positive control. Relative concentrations per secreted factor are depicted by circle size, absolute concentrations per secreted factor is shown by color gradient.

60
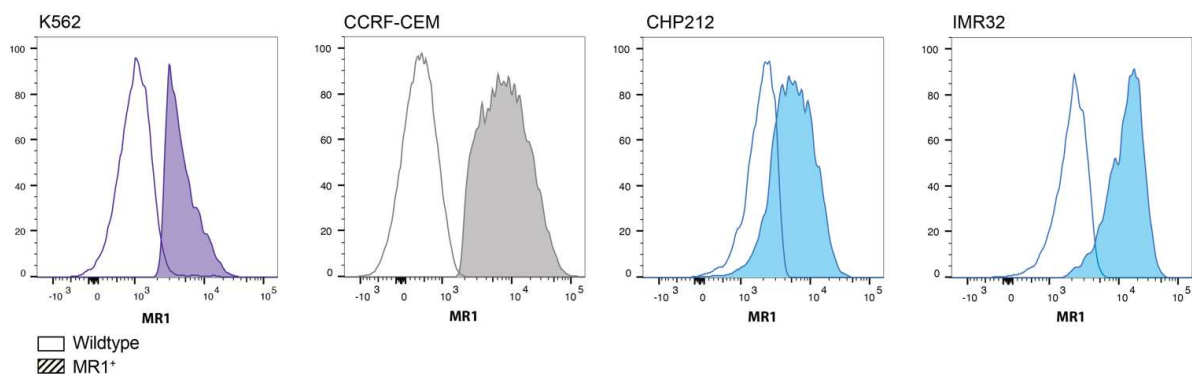
61   **Supplementary Figure 5.** Efficient lentiviral induction of MR1 overexpression.

Supplemental material

BMJ Publishing Group Limited (BMJ) disclaims all liability and responsibility arising from any reliance placed on this supplemental material which has been supplied by the author(s)

J Immunother Cancer

62   *MR1 was overexpressed in K562 (purple, adult positive control) and three MC.7.G5-mediated targeting resistant*

63   *cell lines (1 T-ALL model (Grey, CCRF-CEM) and 2 NBL models (Blue, CHP212 & IMR32). Open: wildtype, filled: MR1*

64   *overexpressing.*

REACTIVE OXYGEN SPECIES (ROS)

	Pathway	NES	Padj	Size
1	GOBP CELLULAR RESPONSE TO REACTIVE OXYGEN SPECIES	-1.52211628579211	0.264327002461165	42
2	GOBP NEGATIVE REGULATION OF REACTIVE OXYGEN SPECIES BIOSYNTHETIC PROCESS	1.13609462301622	0.671021594430943	3
3	GOBP NEGATIVE REGULATION OF REACTIVE OXYGEN SPECIES METABOLIC PROCESS	0.857271078243061	0.86949994714029	10
4	GOBP NEGATIVE REGULATION OF RESPONSE TO REACTIVE OXYGEN SPECIES	-1.20515140759182	0.632105131235006	7
5	GOBP POSITIVE REGULATION OF REACTIVE OXYGEN SPECIES BIOSYNTHETIC PROCESS	-1.3170241884884	0.52881905923135	3
6	GOBP POSITIVE REGULATION OF REACTIVE OXYGEN SPECIES METABOLIC PROCESS	-1.91759575725226	0.0955080935859502	18
7	GOBP POSITIVE REGULATION OF RESPONSE TO REACTIVE OXYGEN SPECIES	-1.22147539182008	0.500606890696664	1
8	GOBP PROGRAMMED CELL DEATH IN RESPONSE TO REACTIVE OXYGEN SPECIES	-0.859511405523052	0.857064568074386	4
9	GOBP REACTIVE OXYGEN SPECIES BIOSYNTHETIC PROCESS	0.855341997399599	0.86949994714029	8
10	GOBP REACTIVE OXYGEN SPECIES METABOLIC PROCESS	-1.72435517765445	0.0945448106928226	51
11	GOBP REGULATION OF REACTIVE OXYGEN SPECIES BIOSYNTHETIC PROCESS	0.846042878044485	0.871518336201051	7
12	GOBP REGULATION OF REACTIVE OXYGEN SPECIES METABOLIC PROCESS	-1.64060221086448	0.198487383238228	35
13	GOBP REGULATION OF RESPONSE TO REACTIVE OXYGEN SPECIES	0.841710592087563	0.874434905110248	13
14	GOBP RESPONSE TO REACTIVE OXYGEN SPECIES	-1.51566325623634	0.185106597750676	55

NUCLEOBASE

	Pathway	NES	Padj	Size
1	GOBP NEGATIVE REGULATION OF NUCLEOBASE CONTAINING COMPOUND METABOLIC PROCESS	1.39565011334921	0.0918406712136247	322
2	GOBP NUCLEOBASE BIOSYNTHETIC PROCESS	-0.709787532258686	0.92118383565752	4
3	GOBP NUCLEOBASE CATABOLIC PROCESS	1.10330128910786	0.683909690888275	1
4	GOBP NUCLEOBASE CONTAINING COMPOUND TRANSPORT	-0.991813527475825	0.771742945221721	45
5	GOBP NUCLEOBASE CONTAINING SMALL MOLECULE BIOSYNTHETIC PROCESS	-1.36606981532798	0.458975981105417	3
6	GOBP NUCLEOBASE CONTAINING SMALL MOLECULE CATABOLIC PROCESS	-0.805995441025804	0.928855477474533	1
7	GOBP NUCLEOBASE CONTAINING SMALL MOLECULE INTERCONVERSION	-1.12561287317706	0.683909690888275	3
8	GOBP NUCLEOBASE CONTAINING SMALL MOLECULE METABOLIC PROCESS	-1.3690524481014	0.244902376392826	130
9	GOBP NUCLEOBASE METABOLIC PROCESS	-1.06540738818404	0.740044691489701	10
10	GOBP NUCLEOBASE TRANSPORT	-1.09799047082221	0.694174643393393	1
11	GOBP POSITIVE REGULATION OF NUCLEOBASE CONTAINING COMPOUND TRANSPORT	-0.618441806889541	0.973870947106773	2
12	GOBP PURINE NUCLEOBASE BIOSYNTHETIC PROCESS	-0.709787532258686	0.92118383565752	4
13	GOBP PURINE NUCLEOBASE METABOLIC PROCESS	-0.996871516799466	0.765674384850001	8
14	GOBP PYRIMIDINE NUCLEOBASE CATABOLIC PROCESS	1.10330128910786	0.683909690888275	1
15	GOBP PYRIMIDINE NUCLEOBASE METABOLIC PROCESS	-0.907538096921615	0.844603523438117	2
16	GOBP REGULATION OF NUCLEOBASE CONTAINING COMPOUND TRANSPORT	-0.848953113681339	0.863563436084988	5

65   **Supplementary Figure 6.** No enrichment of metabolic gene sets implied in formation of antigens recognized by

66   MR1T-cells between targeted HB13F and resistant HB13E organoids.

67   *Differential gene set enrichment analysis was performed on single cell RNA sequencing data[40] of MC.7.G5*

68   *targeted HB13F and MC.7.G5 resistant HB13E HBL organoids grown from the same patient. Enrichment analysis*

69   *in gene sets containing "Reactive Oxygen Species" and "Nucleobase" did not reveal any significant differences*

Supplemental material

BMJ Publishing Group Limited (BMJ) disclaims all liability and responsibility arising from any reliance placed on this supplemental material which has been supplied by the author(s)

J Immunother Cancer

70   *between targeted and resistant cells. Size: number of genes included in gene set. GOBP: gene ontology biological*

71   *process, NES = normalized enrichment score; PAdj = Adjusted P-value.*

72   **Supplementary Tables**

73   **Supplementary Table 1.** Allelic MR1 variants observed in utilized cell lines.

74   *Allelic MR1 variants, extracted from the EnaraBio and CCLE databases Targeting defined as >15% standardized*

75   *killing.*

Sample Name	MR1 Mutation	MR1 Allelic Variant	Targeted?
K562	-	MR1*01	Yes
Jurkat	-	MR1*01	Yes
CHP212	-	MR1*01	No
Kasumi-1	p.H39R	MR1*02	No
CCRF-CEM	p.H39R	MR1*02	No
NALM-6	p.R31H,p.H39R	MR1*04	Yes
MOLT16	-	MR1*01	Yes
697	p.R31H,p.H39R	MR1*04	Yes
RCH-ACV	-	MR1*01	Yes
SUP-B15	-	MR1*01	No

76

77   **Supplementary Table 2.** Characteristics of previously established organoid models.

78   *Characteristics of models established with the respective disease-specific organoid establishing- and culture*

79   *protocols from which basic characteristics are not yet present in literature. HCC: hepatocellular carcinoma, NBL:*

80   *neuroblastoma, MRT: malignant rhabdoid tumor*

Organoid	Disease	Source	Location	Age of patient	Establishing Protocol
pHCC	HCC	Primary Tumor, Biopsy	Liver	10 years	[14,40]
039	NBL	Relapse, Resection	Lymph Node	2 years	[17]
JD041T	MRT	Primary tumor, Resection	Eye	3 years	[18,19]
JD081T	MRT	2nd relapse, primary tumor site, resection	Rectum	4 years	[18,19]

81